Available online at www.sciencedirect.com

ScienceDirect

Mendeleev Commun., 2020, **30**, 174–176

Mendeleev Communications

Adsorption characteristics of nanographite oxide obtained from thermally expanded graphite

Elena Yu. Obraztsova,[a] Marie N. Barshutina,*[b] Evgeny S. Bakunin,[a] Artem V. Rukhov,[a] Anna A. Shipovskaya[a] and Alexey V. Shuklinov[c]

[a] *Tambov State Technical University, 392000 Tambov, Russian Federation*
[b] *St. Petersburg State University, 199034 St. Petersburg, Russian Federation. E-mail: barshutina.marie@yandex.ru*
[c] *G. R. Derzhavin Tambov State University, 392000 Tambov, Russian Federation*

DOI: 10.1016/j.mencom.2020.03.014

Nanographite oxide was synthesized from thermally expanded graphite in an environmentally friendly electrochemical manner, and its adsorption properties were examined in a batch system. Three two-parameter isotherm models (Langmuir, Freundlich, and Dubinin–Radushkevich) were applied for the experimental data processing, and the adsorption kinetics was estimated according to pseudo-first and pseudo-second order simplified kinetic models. The acquired results revealed that obtaned nanographite oxide can be employed as an inexpensive and efficient adsorbent for removal of acidic dyes from aqueous solutions.

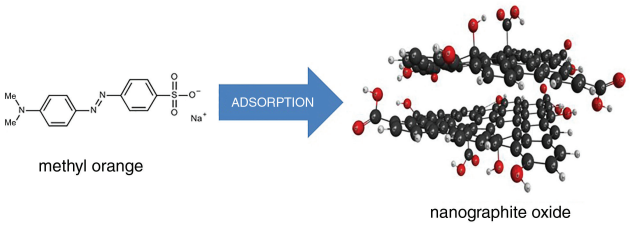

Keywords: nanographite oxide, thermally expanded graphite, methyl orange, adsorption isotherm, adsorption kinetics, diffusion mechanism.

Currently, various types of dyes widely applied in textile, cosmetics, paper and coloring industries have become one of the most serious pollutants of the environment, including drinking water. The majority of them are toxic, non-biodegradable and harmful to both aquatic biosphere and human.[1–3] Many techniques have been proposed for the removal of dyes from aqueous solutions, such as electrochemical oxidation, reverse osmosis, membrane separation, chemical coagulation, biological treatment, and adsorption.[4] At this end, the adsorption approach has been demonstrated as superior in terms of initial cost, efficiency, and simplicity of operation.[5]

An implementation of the adsorption procedure involves adsorbents of the following types: natural adsorbents, agricultural wastes, industrial wastes, biomass, nanocomposites, dendritic polymers, and nanomaterials based on carbon, noble metals, metal oxides, spinel ferrite, *etc*.[6] Among these adsorbents, carbon-based nanomaterials (activated carbon, graphite oxide, and graphene) are of particular interest due to their large specific surface area, high reactivity, and dispersibility. Moreover, the two-dimensional nature, associated band structure, and presence of surface functional groups make single sheets of carbon a promising adsorbent for the water purification.[7,8] To date, the activated carbon is one of the most widely used carbon adsorbents, but its application for the wastewater purification to remove dyes remains quite an expensive process.[9] Hence, there is a growing interest in the development of novel carbon-based adsorbents possessing the advantages of nanosized carbon materials but being low-cost products.

Nanographite oxide (NGO) is a promising material that meets the abovementioned requirements. It has been already employed in many applications, however only few reports have been focused on the nanographite usage in the environmental treatment.[10–12]

The present work was aimed at the investigation of adsorption properties of NGO obtained *via* an electrochemical exfoliation of thermally expanded graphite (TEG)[13] and at the evaluation of its potential effectiveness for the purification of aqueous solutions from dyes. The method used for the NGO preparation differs from the conventional Hummer's method[14] in its simplicity of implementation, efficiency, and environmental safety. Moreover, the use of TEG as a starting material can greatly increase the production yield and influence the porosity of the final product, which significantly affects its adsorption properties.[†] The structure and morphology of NGO samples obtained *via* the electrochemical exfoliation of TEG foil were characterized by scanning electron microscopy (SEM) and IR spectroscopy. The SEM micrograph of NGO has revealed that it possesses a multiple lamellar layered structure with clearly visible edges of individual sheets (Figure S1 in Online Supplementary Materials). It can also be noted that the NGO sheets are thicker at the edges due to the presence of significant amounts of oxygen-containing functional groups. The IR spectrum of the material (Figure S2) contains absorption bands within a range of 3000–3600 cm^{-1}, which can be assigned as stretching vibrations of OH–H bonds. Absorption bands at 1735 cm^{-1} are related to the vibrational bonds of C=O moiety either of ketone or another carbonyl group. The band at 1296 cm^{-1} is

[†] See Online Supplementary Materials for the detailed procedure for NGO production and characterization.

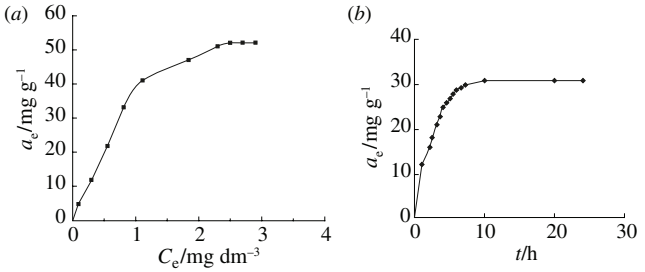

Figure 1 (*a*) Adsorption isotherm for MO onto NGO surface and (*b*) kinetic adsorption curve.

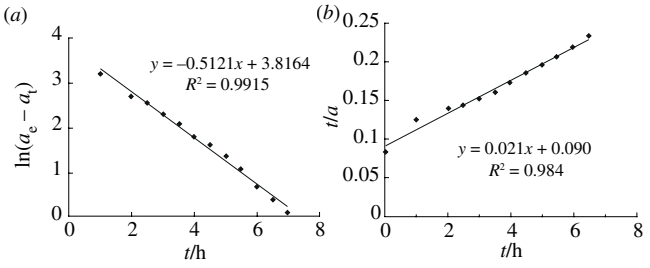

Figure 2 (*a*) Pseudo-first order and (*b*) pseudo-second order kinetics in the NGO–MO system.

characteristic of the C–O vibrations in carboxyl group, and the band at 1164 cm^{-1} belongs to stretching vibrations of the C–OH bond.[15] Functional groups at the edges of nanographite sheets create a negative charge on their surfaces, which leads to a hydrophilicity and a high dispersibility of NGO in polar solvents. The oxygen-containing groups can considerably change the nature of NGO surface from non-polar to polar, and thus enhance the adsorption properties of NGO towards ionic and non-ionic pollutants.

To evaluate a dye adsorption mechanism on the NGO surface, methyl orange (MO) was selected as a dye often used as the model compound for such purposes.[16,17] Figure 1(*a*) shows the adsorption isotherm plotted for the acquired experimental data, revealing the relationship between the amount of adsorbed MO per unit mass of NGO (*i.e.*, the equilibrium adsorption capacity, a_e) and the equilibrium concentration (C_e) of MO in solution.

To gain a further understanding of the mechanism of dye adsorption by NGO, Langmuir, Freundlich and Dubinin–Radushkevich isotherm models[18–20] were employed (Table 1).

According to the acquired data, the Freundlich isotherm model describes the adsorption process in the most appropriate manner with $R^2 = 0.9935$. Therefore, it can be concluded that the MO adsorption by NGO occurs on the heterogeneous surface, and its most active sites possess different energy values, which is apparently due to the presence of different types of functional groups on the NGO surface. The equilibrium adsorption capacity (a_e) was found to be 52 mg g^{-1}.

The experimental data also allowed us to plot the kinetic adsorption curve [Figure 1(*b*)]. According to this curve, the equilibrium in the NGO–MO adsorption system was achieved within 10 h. The pseudo-first and pseudo-second order kinetic models (of Lagergren[21] and Ho,[22] respectively) have been subsequently applied in order to examine the controlling mechanism in this adsorption system. Figure 2 shows the linear representations for both the kinetic adsorption models, and Table 2 summarizes the kinetic parameters calculated according to these models.

According to the obtaned results, the pseudo-first order kinetic model fits better to the experimental data ($R^2 = 0.9935$), which indicates a physical nature of the adsorption processes in the NGO–MO system. However, the determination coefficient for the pseudo-second order model is also quite high (R^2 = = 0.9912), which allows us to suggest that there is an electrostatic interaction between the functional groups located on the surface of NGO, *e.g.*, COOH and the chromophore –N=N group of dye molecule.

To assess the contribution of internal and external diffusion processes to the overall adsorption rate, the experimental kinetic data were processed using the Weber–Morris and Boyd diffusional models.[23,24] Figure 3 shows the kinetic curves of MO adsorption onto NGO, plotted in the coordinates of both models.

The results reveal that the graph plotted within the Weber–Morris coordinates is linear over the whole interval of time with a sufficiently high regression coefficient (R^2 = 0.994), which indicates that intraparticle diffusion is highly involved in the adsorption process. However, the graph constructed within the Boyd coordinates is linear with a much smaller regression coefficient (R^2 = 0.945) and does not pass through the origin, which proves a significant effect of the external diffusion mass transfer on the total adsorption rate. Thus, the acquired results suggest an involvement of both the external and intraparticle diffusion mechanisms in the adsorption of MO by NGO.

In summary, our results confirm that the NGO obtained *via* the electrochemical exfoliation of TEG possesses the substantial adsorption efficiency and can be considered as a promising and an inexpensive adsorbent for the removal of acidic dyes from aqueous media. The method proposed for the NGO production demonstrates a number of significant advantages as compared to the conventional Hummer's method. In particular, our method does not require the use of strong oxidizers and aggressive reagents such as $KMnO_4$, $NaNO_3$, $HClO_4$, concentrated H_2SO_4, *etc*. It is easier to scale and less labor-consuming, does not require the employment of expensive corrosion-resistant equipment, and does not contribute to the generation of toxic and explosive gases such as nitrogen, sulfur and chlorine oxides. Moreover, the NGO obtained *via* the electrochemical exfoliation of TEG possesses the developed heterogeneous surface with active variegated energetic sites, which is beneficial for the NGO adsorption efficiency. The equilibrium adsorption capacity of NGO towards MO was found to be 52 mg g^{-1}, which is comparable with the capacity of many commonly used adsorbents.[25] Finally, the equilibrium adsorption isotherm fits well to the Freundlich isotherm model, indicating a physical nature of the adsorption processes in the NGO–MO system and the absence of adverse chemical reactions in the adsorption process.

Table 1 Coefficients in the isotherm equations.

Equation	Freundlich			Langmuir				Dubinin–Radushkevich		
	$1/n$	K_F	R^2	$1/a_m$	$1/K_L a_m$	K_L	R^2	β	E	R^2
$y = 3.226 + 0.449x$	0.44	25.2	0.9935							
$y = 0.054 + 0.495x$				0.02	0.054	1.48	0.9223			
$y = 3.97 - 6.35x$								6.35	0.8	0.9927

Table 2 Kinetic parameters for the pseudo-first order and pseudo-second order models.

Equation	Pseudo-first order		Pseudo-second order	
	k_1	R^2	k_2	R^2
$y = 3.8164 - 0.5121x$	0.5121	0.9935		
$y = 0.0909 + 0.0213x$			0.032	0.9912

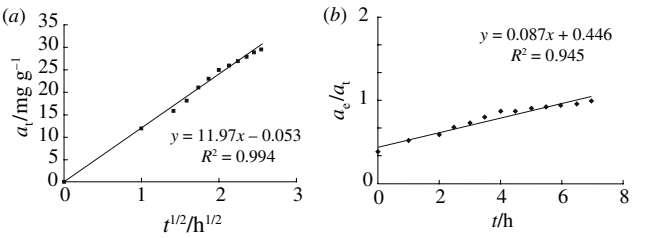

Figure 3 Kinetic curves within the (*a*) Weber–Morris and (*b*) Boyd coordinates.

This work was supported by the Department of Education and Science at the Tambov Region Administration [grant no. 38-MU-19 (02)].

Online Supplementary Materials

Supplementary data associated with this article can be found in the online version at doi: 10.1016/j.mencom.2020.03.014.

References

1 R. Kant, *Nat. Sci.*, 2012, **4**, 22.
2 K.-T. Chung, *J. Environ. Sci. Health, Part C*, 2016, **34**, 233.
3 M. A. Hassaan and A. El Nemr, *Am. J. Environ. Sci. Eng*., 2017, **1**, 64.
4 A. Ahmad, S. H. Mohd-Setapar, C. S. Chuong, A. Khatoon, W. A. Wani, R. Kumar and M. Rafatullah, *RSC Adv*., 2015, **5**, 30801.
5 R. K. Vital, K. V. N. Saibaba, K. B. Shaik and R. Gopinath, *J. Biorem. Biodegrad*., 2016, **7**, 371.
6 N. B. Singh, G. Nagpal, S. Agrawal and Rachna, *Environ. Technol. Innov*., 2018, **11**, 187.
7 K. S. Rao, M. Mohapatra, S. Anand and P. Venkateswarlu, *Int. J. Eng. Sci. Technol*., 2010, **2**, 81.
8 I. Sheet, A. Kabbani and H. Holail, *Energy Procedia*, 2014, **50**, 130.
9 M. M. Hassan, C. J. Hawkyard, in *Environmental Aspects of Textile Dyeing*, ed. R. M. Christie, Woodhead Publishing, 2007, ch. 7, pp. 149–190.
10 W. Li, X. Lin, M. Yu, I. Mubeen, A. Buekens and X. Li, *Aerosol Air Qual. Res*., 2016, **16**, 3281.
11 C. Li, Y. Dong, J. Yang, Y. Li and C. Huang, *J. Mol. Liquids*, 2014, **196**, 348.
12 B. Zhang, F. Li, T. Wu, D. Sun and Y. Li, *Colloids Surf., A*, 2015, **464**, 78.
13 E. Yu. Obraztsova, A. A. Degtyarev, A. V. Rukhov and E. S. Bakunin, *Vestnik TSTU*, 2019, **25**, 116 (in Russian).
14 W. S. Hummers, Jr. and R. E. Offeman, *J. Am. Chem. Soc.*, 1958, **80**, 1339.
15 S. A. Khan, S. B. Khan, L. U. Khan, A. Farooq, K. Akhtar and A. M. Asiri, in *Handbook of Materials Characterization*, ed. S. K. Sharma, Springer, Cham, 2018, ch. 9, pp. 317–344.
16 J. Pal, M. K. Deb, D. K. Deshmukh and D. Verma, *Appl. Water Sci*., 2013, **3**, 367.
17 G. U. Nandhini, K. Arivalagan and S. Sivanesan, *Int. J. Trend Sci. Res. Dev*., 2017, **2**, 1550.
18 H. M. F. Freundlich, *J. Chem. Phys*., 1906, **57**, 385.
19 I. Langmuir, *J. Am. Chem. Soc.*, 1918, **40**, 1361.
20 M. M. Dubinin and L. V. Radushkevich, *Dokl. Akad. Nauk SSSR*, 1947, **55**, 331 (in Russian).
21 S. Y. Lagergren, *K. Sven. Vetenskapsakad. Handl.,* 1898, **24**, 1.
22 Y. S. Ho and G. McKay, *Process Biochem*., 1999, **34**, 451.
23 G. E. Boyd, A. W. Adamson and L. S. Myers, Jr., *J. Am. Chem. Soc.*, 1947, **69**, 2836.
24 W. J. Weber, Jr. and J. C. Morris, *J. Sanit. Eng. Div*., *Am. Soc. Civ. Eng.*, 1963, **89**, 31.
25 M. R. Samarghandi, M. Hadi, S. Moayedi and F. B. Askari, *Iran. J. Environ. Health Sci*. *Eng*., 2009, **6**, 285.

Received: 17th October 2019; Com. 19/6042